

# Joint Performance Analysis of Channel Quality Indicator Feedback Schemes and Frequency-Domain Scheduling for LTE

Sushruth N. Donthi and Neelesh B. Mehta, *Senior Member, IEEE*

**Abstract**—Frequency-domain scheduling and rate adaptation enable next generation orthogonal frequency division multiple access (OFDMA) cellular systems such as Long Term Evolution (LTE) to achieve significantly higher spectral efficiencies. LTE uses a pragmatic combination of several techniques to reduce the channel state feedback required by a frequency-domain scheduler. In the subband-level feedback and user selected subband feedback schemes specified in LTE, the user reduces feedback by only reporting the channel quality averaged over groups of resource blocks called subbands; this leads to an occasional incorrect determination of rate by the scheduler for some resource blocks. In this paper, we develop closed-form expressions for the throughput achieved by the feedback schemes of LTE. The analysis quantifies the joint effects of three critical components on the overall system throughput, namely, scheduler, multiple antenna mode, and feedback scheme, and brings out its dependence on system parameters such as number of resource blocks per subband and the rate adaptation thresholds. The effect of the coarse subband-level frequency granularity of feedback is captured. The analysis provides an independent theoretical reference and a quick system parameter optimization tool to an LTE system designer, and also helps theoretically understand the behavior of OFDMA feedback reduction techniques when operated under practical system constraints.

**Index Terms**—Long Term Evolution (LTE), Channel quality feedback, Multiple antenna diversity, Scheduling, Rate adaptation, Orthogonal frequency division multiple access (OFDMA).

## I. INTRODUCTION

Frequency-domain scheduling enables high spectral efficiencies in next generation wireless cellular standards such as Long Term Evolution (LTE) [1], [2] and IEEE 802.16e/m (WiMAX), both of which employ orthogonal frequency division multiple access (OFDMA). Multiple antenna techniques increase their spectral efficiency even further.

In order to schedule in the frequency domain, the base station (BS) ideally needs to know the instantaneous channel state information (CSI) for the several hundred subcarriers for each of the users (UEs) it is serving. Each user needs to feed back its CSI to the BS when the uplink and downlink channels are not reciprocal. This is so for the popular frequency division

duplex (FDD) mode of operation in LTE, which is the focus of this paper.<sup>1</sup>

Given the large number of subcarriers, such extensive subcarrier-level feedback is practically infeasible and inefficient as it consumes significant uplink bandwidth. Hence, a balance must be struck between gains possible from multiuser diversity and the amount of feedback required to achieve it. Given the practical importance of OFDMA, several feedback reduction techniques have been studied in the literature. In [3], every user feeds back CSI only for the subcarriers whose channel gains exceed a certain threshold. In [4], the overhead is reduced further by making each user feed back only one bit per subcarrier and only for subcarriers whose channel gains exceed a threshold. Such thresholding was further combined with subcarrier grouping in [5]. An alternate approach was pursued in [6], [7] in which each user only sends the gains of a pre-specified number of subcarriers with the highest gains.

In a practical system such as LTE, a pragmatic combination of several of the above techniques is used in order to achieve a significant reduction in the feedback overhead. In LTE, the CSI is quantized into a 4-bit value called channel quality indicator (CQI). Further, only the average CSI observed over a subband, which is a large group of 24 to 96 subcarriers, is reported in the CQI. While the frequency resolution of the CQI fed back is a subband, the BS can assign at the finer granularity of a physical resource block (PRB), which is a group of 12 subcarriers. Three feedback mechanisms are specified in LTE, namely, *wideband feedback*, *UE selected subband feedback*, and *subband-level feedback*. Briefly, in wideband feedback, only one CQI value is reported by each UE for the entire bandwidth. In subband-level feedback, one CQI value is reported by each UE for every subband. In UE selected subband feedback, each UE sends the indices of its best  $M$  subbands and just one average CQI value for all the selected subbands.

In addition to the feedback scheme, the system throughput also depends on the scheduler used by the BS as it determines which user is assigned to each PRB. For example, limiting the feedback has a relatively marginal impact on the performance of a round-robin (RR) scheduler, which does not use the CQI to determine which user to assign to which PRB. On the other hand, the performance of the greedy scheduler [4], [7] and the proportional fair (PF) scheduler [7],[8, Sec. 6.7.1],[9], [10] does depend on the resolution of the CQI as they use it to

The authors are with the Dept. of Electrical Communication Eng. at the Indian Institute of Science (IISc), Bangalore, India.

Emails: dnsushruth@gmail.com, nbmehta@ece.iisc.ernet.in

This work was partially supported by a project funded by the Ministry of Information Technology, India.

A part of this work has been presented at the National Conf. on Communications (NCC) 2010 and the IEEE Global Communications Conf. (Globecom) 2010.

<sup>1</sup>The same also applies to the time division duplex (TDD) mode when the uplink interference and downlink interference are asymmetric.

determine which user is assigned to each PRB. While the greedy scheduler maximizes system throughput at the expense of fairness, the PF scheduler ensures fairness among users by also accounting for the average rates experienced by the users.

### A. Focus and Contributions of The Paper

In this paper, we analyze the performance of CQI feedback schemes of LTE that enable frequency-domain scheduling. To this end, we develop closed-form expressions for the throughput of the PF and greedy schedulers for the *UE selected subband feedback* and *subband-level feedback* schemes. The RR scheduler, where applicable, is also analyzed in order to quantify the gains from frequency-domain scheduling. Besides covering a wide range of schedulers, the analysis also accounts for the many diversity-based multiple antenna modes supported by LTE, such as single input multiple output (SIMO), open-loop and closed-loop multiple input single output (MISO), and single-stream multiple input multiple output (MIMO). Altogether, the analysis quantifies the joint effects of the three critical components, namely, scheduler, multiple antenna mode, and quantized CQI feedback scheme, on the overall throughput. These have hitherto been understood either qualitatively or through simulations.

Given the global deployment envisaged for LTE, such an analysis is both practically relevant and theoretically interesting, as it helps better understand and improve the system performance. For example, the analysis quantifies how the coarse frequency granularity of the feedback can lead to an occasional incorrect determination of the appropriate MCS, which reduces the overall throughput. The link adaptation thresholds, therefore, should be chosen to also account for this additional source of error. This is new when compared to the conventional rate adaptation problem [11], in which the adaptation thresholds are directly determined from the block error rate curves. The analytical expressions also enable a system designer to determine the optimum value of  $M$  for the UE selected subband feedback scheme as a function of the scheduler and multiple antenna mode.

In order to facilitate the analysis, the paper first develops a model of the CQI feedback schemes that balances the conflicting demands of being analytically tractable and yet modeling, as closely as possible, all the relevant mechanisms in the standard. This problem becomes especially difficult when one studies a technology as rich as LTE, which employs a combination of several schemes proposed in the literature. Further, the paper also develops several novel approximations.

Given the modeling and analytical complexity of the problem, the LTE-specific literature that deals with either scheduling algorithms or limited feedback has often been simulation based [9], [10], [12]. For example, in [10], contiguous and distributed subcarrier allocations are compared and their effects on the throughput of greedy and PF schedulers is analyzed. In [9], the performance of PRB-level feedback schemes was studied for a PF scheduler. An analysis was developed in [13] for a scheme in which each user feeds back the indices of a pre-specified number of subcarriers with the highest gains and the BS uses BPSK modulation and a RR scheduler to

transmit. However, rate adaptation, multiple antenna diversity, the coarse frequency granularity of feedback, and channel-aware frequency-domain scheduling were not modeled. The analysis in [14] quantified the performance gains of MIMO in a cellular system. However, OFDMA – and, consequently, all its frequency-domain aspects – was not modeled. While the performance of a greedy scheduler in a generic MIMO-OFDM system that uses orthogonal space-frequency block codes was analyzed in [15], the model assumed one-bit feedback and did not consider the coarse frequency granularity of feedback.

The paper is organized as follows. We first review the LTE frame structure and its feedback schemes in Sec. II. This motivates the system model in Sec. III and leads to its analysis in Sec. IV. Numerical results and conclusions follow in Sec. V and Sec. VI, respectively.

## II. OVERVIEW OF LTE FRAME STRUCTURE AND CQI FEEDBACK

In LTE, each downlink *frame* is 10 ms long and consists of ten subframes, each of duration 1 ms. A subframe consists of two 0.5 ms slots, with each slot containing seven OFDM symbols. In the frequency domain, the system bandwidth,  $B$ , is divided into several subcarriers, each of bandwidth of 15 kHz. A set of twelve consecutive subcarriers for a duration of one slot is called a *Physical Resource Block (PRB)*.

*Channel Quality Indicator (CQI) Feedback:* The CQI is a 4-bit value that indicates an estimate of the modulation and coding scheme (MCS) that the UE can receive reliably from the BS. It is typically based on the measured received signal quality, which can be estimated, for example, using the pilots sent by the BS on the downlink. The  $2^4 = 16$  MCSs and their rates are tabulated in [16, Tbl. 7.2.3-1].

The BS controls how often and when the UE feeds back CQI. The finest possible frequency resolution for CQI reporting is a subband, which consists of  $q$  contiguous PRBs. Depending on the system bandwidth and the feedback scheme,  $q$  ranges from 2 to 8. The BS can make a UE report CQI using one of three different feedback schemes: (i) In *wideband feedback*, the UE reports only one wideband CQI value for the whole system bandwidth. (ii) In *subband-level feedback*, the UE reports the CQI for each subband. (iii) In *UE selected subband feedback*, the UE reports the position of the  $M$  subbands that have the highest CQIs and only a single CQI value that indicates the channel quality when averaged over all these  $M$  subbands.<sup>2</sup>

*Multiple Antennas at BS and UE:* We focus on single-stream transmission in this paper in order to not involve design issues related to feedback of the precoding matrix indicator and rank indicator variables. This encompasses the following modes of operation: single input single output (SISO) ( $N_t = N_r = 1$ ), SIMO ( $N_t = 1$  and  $N_r \geq 2$ ), closed-loop and open-loop MISO ( $N_t \geq 2$  and  $N_r = 1$ ), and single-stream MIMO ( $N_t \geq$

<sup>2</sup>LTE further reduces the CQI overhead in both the subband-level and UE selected subband feedback as follows. A UE reports a 2-bit differential CQI value for each subband and a wideband CQI value for the whole system bandwidth. We shall ignore the minor impact of the differential nature of feedback.

2 and  $N_r \geq 2$ ). Larger values of  $N_t$  and  $N_r$  can also be considered.

*PRB Allocation and Signaling:* Based on the CQI reports from all the UEs, the scheduler in the BS decides which PRB to allocate to which UE. The scheduler is not specified in the standard and is implementation-dependent. Based on the scheduler's decision, the BS uses one of the three *Resource Allocation Types* specified in LTE to signal, on the downlink control channel, the specific PRBs that are allocated to different UEs. These three allocation types trade off the control signaling overheads in slightly different ways. *Note that the smallest block of frequency that can be allocated to a UE is a PRB. However, this allocation is based on CQI feedback, which has a coarser subband-level frequency resolution.*

### III. SYSTEM MODEL

Our goal is to analyze the system throughput of the subband-level and UE selected subband CQI reporting schemes. The wideband CQI scheme is not of interest as it does not support frequency-domain scheduling. We develop the analysis for the following system model, which faithfully captures the LTE standard described in the previous section and, yet, is analytically tractable. This is made possible by the judicious use of some modeling simplifications and analytical approximations, which are mentioned and justified below. Without such simplifications, the only option would be extensive simulations.

Let a BS serve  $K$  users and let  $N$  be the total number of PRBs available. The total number of subbands is  $S = \lceil N/q \rceil$ , where  $\lceil \cdot \rceil$  denotes the ceil function. The BS is equipped with  $N_t$  transmit antennas and each UE has  $N_r$  receive antennas. The channel between each antenna pair between the BS and a UE is assumed to undergo block Rayleigh fading, and remains constant over a 1 ms subframe. For any UE, the channel gain of the 12 subcarriers within a PRB is the same. The channel gains across different PRBs are assumed to be independent and identically distributed (i.i.d.), as has also been assumed in [4], [13], [17]–[20]. It is a valid assumption when the coherence bandwidth of the channel is close to the 180 kHz bandwidth of a PRB [2, Sec. 5.3.2]. It is needed in the analysis because the CQI generated is averaged across PRBs. The channel gains are assumed to be i.i.d. across different antenna pairs for all users, as has also been assumed in [14], [21]–[23]. This is valid when the antennas are spaced at least half a wavelength apart in a rich scattering environment. We shall also investigate the impact of space and frequency correlations on the throughput in Sec. V-C, which presents simulation results for some standardized channel models.

Let  $h_{n,k}(i, j)$  denote the channel gain from the  $j^{\text{th}}$  transmit antenna to the  $i^{\text{th}}$  receive antenna of the  $k^{\text{th}}$  UE for the  $n^{\text{th}}$  PRB. Thus, it is i.i.d. across the antenna indices  $i$  and  $j$  and across the PRB index  $n$ . It is a zero-mean complex Gaussian random variable (RV) with variance  $\sigma_k^2$ , which depends upon shadowing and the distance of UE  $k$  from the BS. Hence, it is independent but not identically distributed across  $k$ .

Note that the CQI value fed back by the UE depends on the antenna mode being used. In LTE, the UE feeds back CQI for one antenna mode, which is chosen a priori by the eNodeB and

UE, *e.g.*, at the time of connection establishment. Since this paper focuses on single-stream transmissions, the choice of the multiple antenna scheme to use is governed by the number of antennas available at the BS and UE. For example, if  $N_t = N_r = 2$ , the system would prefer the single-stream MIMO scheme over others since it gives a better throughput.<sup>3</sup>

As can be seen, the description of the physical layer of LTE and its feedback mechanisms is quite involved. In order to make the problem analytically tractable and, at the same time, bring out the impact of the different CQI feedback techniques and their interaction with the scheduler, the following simplifying approximations are necessary. Even with the above assumptions, the model is rich, challenging, and relevant. (i) Co-channel interference, if any, from adjacent BSs is assumed to be Gaussian. While [25] does analyze modulation techniques in non-Gaussian interference, an analytically tractable approach for LTE remains an open problem. (ii) Since our focus is on the analysis of the CQI feedback mechanisms, we assume for closed-loop MISO and MIMO that the precoding matrix indicator (PMI) feedback is ideal. As the simulations in [26] show, quantization of transmit beamforming weights typically incurs an additional 10% loss in throughput for  $N_r = N_t = 2$ . Clearly, no such assumption is required for SISO, SIMO, and open-loop MISO. (iii) While all the RBs assigned to a UE use the same MCS in LTE, we assume that different RBs assigned to a UE can use different MCSs. The simulations in [27] show that the difference in throughput between the two is less than 5%. Another implication of this assumption is that channel coding is done per PRB and is not across all PRBs, which would have yielded a small coding gain. (iv) The CQI feedback delays are assumed to be negligible. This is valid for pedestrian speeds, in which the channel coherence time is greater than CQI feedback delays, which are of the order of 6-10 ms. The feedback is assumed to be error-free. Analyzing the impact of feedback errors on the performance of LTE is an open problem.

*Notation:* The received SNR in a subframe for UE  $k$  in the  $n^{\text{th}}$  PRB is denoted by  $\gamma_{n,k}$ . Let  $r_i$  denote the rate in bits/symbol achieved by using the MCS corresponding to the  $i^{\text{th}}$  CQI value. For the subband-level feedback scheme, let  $C_{s,k}^{\text{sub}}$  denote the CQI value reported by UE  $k$  for the subband  $s$ . It can take one of  $L = 16$  possible values. For ease of explanation, we shall no longer distinguish between  $r_i$  and its 4-bit index  $i$  (where  $1 \leq i \leq L$ ), and shall just say that a UE reports a CQI index of  $C_{s,k}^{\text{sub}} = r_i$  for the subband  $s$ . Similarly, for the UE selected subband feedback scheme, let  $C_k^{\text{bestM}}$  denote the single CQI value reported by UE  $k$ . If UE  $k$  reports a CQI value  $i$ , then  $C_k^{\text{bestM}} = r_i$ . Since the PRBs of a user are statistically identical, we focus on the  $n^{\text{th}}$  PRB, unless specified otherwise.

We shall denote the expectation of an RV  $X$  by  $E[X]$  and the probability of an event  $A$  by  $\Pr(A)$ . Similarly,  $E[X|A]$  denotes the conditional expectation given  $A$  and  $\Pr(B|A)$

<sup>3</sup>In high mobility scenarios, however, the BS may prefer to use the open-loop MISO scheme, since the feedback may get outdated. The interested reader is referred to [24] for a framework that adaptively switches between spatial multiplexing and beamforming schemes depending on the channel estimation error.

denotes the conditional probability of  $B$  given  $A$ . For a set  $\mathcal{I}$ ,  $|\mathcal{I}|$  shall denote its cardinality.

#### A. UE Selected Subband CQI Feedback

The CQI is calculated using the subband SNR as follows. The subband SNR,  $\gamma_{s,k}^{\text{sub}}$ , of the  $k^{\text{th}}$  user for subband  $s$  is the average SNR (in linear scale) over its constituent PRBs and is given by [28]<sup>4</sup>:

$$\gamma_{s,k}^{\text{sub}} = \frac{1}{q} \sum_{n \in \mathcal{PRB}(s)} \gamma_{n,k}, \quad (1)$$

where  $\mathcal{PRB}(s)$  denotes the set of PRBs in subband  $s$ .

In UE selected subband feedback, UE  $k$  orders the subband SNRs of its  $S$  subbands as

$$\gamma_{(1),k}^{\text{sub}} \geq \dots \geq \gamma_{(M),k}^{\text{sub}} \geq \dots \geq \gamma_{(S),k}^{\text{sub}},$$

where, using order statistics notation,  $(i)$  is the index of the subband with the  $i^{\text{th}}$  largest SNR. It reports the set  $\mathcal{I}_k = \{(1), \dots, (M)\}$ , which consists of the  $M$  subbands with the highest CQIs. As described in Sec. II, UE  $k$  also reports a single CQI,  $C_k^{\text{bestM}}$ . It depends on the SNR,  $\gamma_k^{\text{rep}}$ , which is obtained by averaging over its  $M$  selected subbands:

$$\gamma_k^{\text{rep}} = \frac{1}{M} \sum_{i=1}^M \gamma_{(i),k}^{\text{sub}}. \quad (2)$$

Based on  $\gamma_k^{\text{rep}}$ , the CQI is reported as

$$C_k^{\text{bestM}} = r_i, \quad \text{if } \gamma_k^{\text{rep}} \in [T_{i-1}, T_i).$$

Here,  $T_0, \dots, T_L$  are the set of link adaptation thresholds that ensure that a target block error rate of 10% is met should the BS transmit over the entire subband [1][2, Fig. 10.1].

1) *Scheduling for UE Selected Feedback*: The BS uses  $\mathcal{I}_k$  and  $C_k^{\text{bestM}}$  reported by all the  $K$  UEs to determine which user to assign to each PRB. This allocation also depends on the scheduler used by the BS. As mentioned, we shall consider the greedy, PF, and RR schedulers.

The greedy and PF schedulers are defined as follows. Let  $s$  denote the subband that contains PRB  $n$ . Let  $\mathcal{Z}$  denote the subset of UEs that have reported the subband  $s$  as one of their best  $M$  subbands. Let the  $n^{\text{th}}$  PRB get assigned to UE  $k^*$ . The assignment rule is as follows:

- *Greedy scheduler*: The  $n^{\text{th}}$  PRB gets assigned to the UE that reports the highest CQI value among the UEs that selected subband  $s$ , i.e.,

$$k^* = \arg \max_{k \in \mathcal{Z}} C_k^{\text{bestM}}. \quad (3)$$

If multiple users have the same highest value of  $C_k^{\text{bestM}}$ , then one of them is chosen with uniform probability.

<sup>4</sup>Alternate averaging methods such as effective exponential SNR for determining the average CQI value also exist [29]. However, these are analytically intractable and are beyond the scope of this paper. Even the approach in [29] leads to rather involved expressions for the moment generating function and the moments of EESM. However, the probability density function (PDF) of EESM remains to be characterized in an analytically tractable closed-form.

- *PF scheduler*: The  $n^{\text{th}}$  PRB is assigned to UE  $k^*$  if [7], [19], [21]

$$k^* = \arg \max_{k \in \mathcal{Z}} \frac{C_k^{\text{bestM}}}{E[C_k^{\text{bestM}}]}. \quad (4)$$

Here also, if multiple users have the same highest value of  $\frac{C_k^{\text{bestM}}}{E[C_k^{\text{bestM}}]}$ , then one of them is chosen with uniform probability. Thus, a PRB gets assigned to the UE whose CQI exceeds its mean rate the most. This ensures fairness across users with different mean rates. Note that this metric is slightly different from that in [30], which uses a moving window average of rate instead of  $E[C_k^{\text{bestM}}]$  in the denominator of (4).

The BS then transmits data on PRB  $n$  to UE  $k^*$  at a rate  $C_{k^*}^{\text{bestM}}$ . Note that for the UE selected feedback scheme, the RR scheduler is not suitable because it allocates PRBs to UEs sequentially and might allocate a PRB  $n$  to a UE that has not selected the subband  $s$ .

*Outage*: Since the CQI value corresponds to the average SNR for the best  $M$  subbands, the actual SNR for the  $n^{\text{th}}$  PRB may be below the lower threshold of the MCS being used. This causes an outage, and the throughput is 0 in that subframe. Outage for PRB  $n$  also occurs if  $\mathcal{Z}$  is a null set since the PRB is then not allocated to any UE.

#### B. Subband-Level CQI Feedback and Scheduling

In subband-level CQI feedback, for every subband  $s$ , each UE  $k$  reports a CQI,  $C_{s,k}^{\text{sub}}$ , based on  $\gamma_{s,k}^{\text{sub}}$ . The CQI is reported as  $C_{s,k}^{\text{sub}} = r_i$  if  $\gamma_{s,k}^{\text{sub}} \in [T_{i-1}, T_i)$ . The BS uses  $C_{s,k}^{\text{sub}}$  reported by all UEs to allocate the PRBs in subband  $s$ . The greedy scheduler assigns PRB  $n$  to UE  $k^*$  if

$$k^* = \arg \max_{1 \leq k \leq K} \{C_{s,k}^{\text{sub}}\}. \quad (5)$$

And, the PF scheduler assigns PRB  $n$  to UE  $k^*$  if

$$k^* = \arg \max_{1 \leq k \leq K} \frac{C_{s,k}^{\text{sub}}}{E[C_{s,k}^{\text{sub}}]}. \quad (6)$$

Note that for both the schedulers, the metric now depends on the subband  $s$  as well. The BS then transmits data on PRB  $n$  to UE  $k^*$  at a rate  $C_{s,k^*}^{\text{sub}}$ . As before, if multiple users have the same highest value of the metric, then one of them is chosen randomly.

For the RR scheduler, each UE is allocated the PRB  $n$  in a cyclic manner, i.e.,  $k^* = 1$  in the first subframe,  $k^* = 2$  in the second subframe, and so on. The process repeats after every  $K$  subframes. Thus,  $C_{s,k}^{\text{sub}}$  only determines the rate to the UE  $k$  and not which PRBs are assigned to it.

*Outage*: As before, an outage occurs if the actual SNR for the  $n^{\text{th}}$  PRB is less than the lower threshold of the MCS used for it.

## IV. ANALYSIS

The statistics of the SNR of PRB  $n$  of UE  $k$ ,  $\gamma_{n,k}$ , shall play a crucial role in the analysis as the CQI that is reported is calculated using it. We present below a single unified characterization of the PDF of  $\gamma_{n,k}$  for SISO, SIMO, open-loop and closed-loop MISO, and single-stream MIMO, and use it to analyze all the multiple antenna modes in one go.

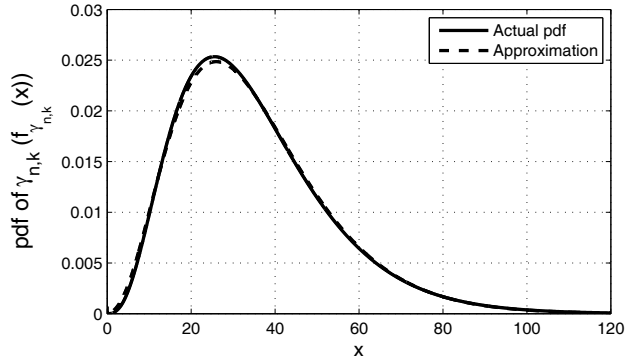


Fig. 1. Plot of the actual and approximate PDFs of  $\gamma_{n,k}$  for single-stream MIMO ( $\sigma_k^2 = 10$  dB).

### A. Common Distribution for $\gamma_{n,k}$

For SIMO ( $N_t = 1$ ,  $N_r = 2$ ), the receiver employs maximal-ratio combining (MRC) [8, Chp. 3]. Hence,  $\gamma_{n,k}$  is a chi-square RV with  $\tau = 2N_r$  degrees of freedom and mean  $N_r\sigma_k^2$ . Clearly, SISO is a special case of SIMO with  $N_r = 1$ . For open-loop MISO ( $N_t = 2$ ,  $N_r = 1$ ), the Alamouti code is used. Therefore,  $\gamma_{n,k}$  is again a chi-square RV with  $\tau = 2N_t$  degrees of freedom and mean  $N_t\frac{\sigma_k^2}{2}$ . For closed-loop MISO, as mentioned in Sec. III, we assume ideal PMI feedback. This is equivalent to assuming that the transmitter employs maximal ratio transmission for every PRB. Then,  $\gamma_{n,k}$  is again a chi-square RV with  $\tau = 2N_t$  and mean  $N_t\sigma_k^2$ .

For single-stream MIMO ( $N_t = N_r = 2$ ),  $\gamma_{n,k}$  is the square of the largest singular value of the matrix  $\{h_{n,k}(i, j)\}_{i,j}$  and its PDF is given by [31, Thm. 2.17] as  $f_{\gamma_{n,k}}(x) = \frac{1}{\sigma_k^2} \left( \left( \frac{x}{\sigma_k^2} \right)^2 - \frac{2x}{\sigma_k^2} + 2 \right) e^{-\frac{x}{\sigma_k^2}} - \frac{2}{\sigma_k^2} e^{-\frac{2x}{\sigma_k^2}}$ , where  $m_1 = E[\gamma_{n,k}] = 3.5\sigma_k^2$  and  $m_2 = E[\gamma_{n,k}^2] = 15.5\sigma_k^4$ . For small  $x$ ,  $f_{\gamma_{n,k}}(x) = \frac{x^3}{3\sigma_k^2} + O(x^4)$ . This is the same as the PDF, for small  $x$ , of a standard chi-square RV with 8 degrees of freedom whose PDF is  $\frac{1}{96}x^3e^{-\frac{x}{2}} \approx \frac{x^3}{96} + O(x^4)$ . This observation motivates the following approximation:

$$\gamma_{n,k} \approx \left( \sqrt{\tau \frac{m_2 - m_1^2}{2}} \right) X_\tau + \left( m_1 - \tau \sqrt{\frac{m_2 - m_1^2}{2\tau}} \right), \quad (7)$$

where  $X_\tau$  is a standard chi-square RV with  $\tau = 8$  degrees of freedom. The scaling factors in (7) are obtained by matching the first and second moments of  $\gamma_{n,k}$  in (7) with those of its actual PDF. Figure 1 plots the actual and the approximate PDFs of  $\gamma_{n,k}$  for  $\sigma_k^2 = 6$  dB, and shows that it is quite accurate. A similar match was also observed for other values of  $\sigma_k^2$ .

Then, for all the four multi-antenna diversity modes,  $\gamma_{n,k}$  can be written as

$$\gamma_{n,k} = aX_\tau + b, \quad (8)$$

where  $X_\tau$  is a standard chi-square RV with  $\tau$  degrees of freedom. Its PDF is given by

$$f_{X_\tau}(x) = \frac{x^{\frac{\tau}{2}-1} e^{-\frac{x}{2}}}{2^{\frac{\tau}{2}} \Gamma(\frac{\tau}{2})}, \quad x \geq 0, \quad (9)$$

TABLE I

PARAMETERS CHARACTERIZING THE PDF OF THE SNR OF PRB  $n$  OF UE  $k$  FOR SISO, SIMO, MISO, AND MIMO,  $\gamma_{n,k} = aX_\tau + b$ .

	$\tau$	$a$	$b$
SISO	2	$\frac{\sigma_k^2}{2}$	0
SIMO	$2N_r$	$\frac{\sigma_k^2}{2}$	0
MISO (closed-loop)	$2N_t$	$\frac{\sigma_k^2}{2}$	0
MISO (open-loop)	$2N_t$	$\frac{\sigma_k^2}{4}$	0
Single-stream MIMO	8	$\sqrt{\frac{m_2 - m_1^2}{2\tau}} \sigma_k^2$ $= 0.451\sigma_k^2$	$m_1 - \tau \sqrt{\frac{m_2 - m_1^2}{2\tau}}$ $= -0.106\sigma_k^2$

where  $\Gamma$  is the Gamma function [32]. The values of  $\tau$ ,  $a$ , and  $b$  are tabulated in Tbl. I. Notice that  $a$  is proportional to  $\sigma_k^2$  and  $b \leq 0$ .

### B. UE Selected Subband Scheme

We now derive expressions for the throughputs of the greedy and PF schedulers. As explained before, the RR scheduler is not suitable for this feedback scheme and is not considered. The following claims shall lead us to the final result for the throughput in (15).

**Claim 1:** Let UE  $k$  be selected for the  $n^{\text{th}}$  PRB and let  $r_i$  be the CQI value that it reports. Then, the conditional probability that  $\gamma_{n,k}$  is less than  $T_{i-1}$  is

$$\begin{aligned} & \Pr(\gamma_{n,k} < T_{i-1} | C_k^{\text{bestM}} = r_i, k \text{ is sel. for } n^{\text{th}} \text{ PRB}) \\ & \approx \frac{\left( \frac{Mq\tau}{2} - 1 \right)! \frac{Mq-1}{2} \tau^{-1}}{\left( \frac{\tau}{2} - 1 \right)!} \sum_{l=0}^{\frac{Mq-1}{2} \tau - 1} \frac{(-1)^l (T_{i-1} - b)^{\frac{\tau}{2} + l}}{\left( \frac{\tau}{2} + l \right)! \left( \frac{Mq-1}{2} \tau - l - 1 \right)! (2a)^{\frac{\tau}{2} + l}} \\ & \times \left[ \frac{\varpi \left( \frac{Mq-1}{2} \tau - l, \frac{MqT_{i-1} - (Mq-1)b}{2a} \right)}{\varpi \left( \frac{Mq\tau}{2}, \frac{Mq}{2a} (T_i - b) \right) - \varpi \left( \frac{Mq\tau}{2}, \frac{Mq}{2a} (T_{i-1} - b) \right)} \right. \\ & \left. - \frac{\varpi \left( \frac{Mq-1}{2} \tau - l, \frac{MqT_{i-1} - (Mq-1)b}{2a} \right)}{\varpi \left( \frac{Mq\tau}{2}, \frac{Mq}{2a} (T_i - b) \right) - \varpi \left( \frac{Mq\tau}{2}, \frac{Mq}{2a} (T_{i-1} - b) \right)} \right], \quad (10) \end{aligned}$$

where  $\varpi(k, x)$  is the Incomplete Gamma function [32, Chp. 6].

*Proof:* The proof is relegated to Appendix A. ■

We shall refer to the above conditional probability as the outage probability in the rest of the paper.

**Claim 2:** The probability that UE  $k$  reports a CQI of  $r_i$  is

$$\Pr(C_k^{\text{bestM}} = r_i) = \Pr(C_k^{\text{bestM}} \leq r_i) - \Pr(C_k^{\text{bestM}} \leq r_{i-1}), \quad (11)$$

where, for  $1 \leq i \leq L$ ,

$$\begin{aligned} & \Pr(C_k^{\text{bestM}} \leq r_i) \approx \frac{1}{\beta} \\ & \times \int_0^{\frac{Mq}{a}(T_i - b)} \frac{z^{\frac{Mq\tau}{2} - 1} e^{-\frac{z}{2}}}{2^{\frac{Mq\tau}{2}} \left( \frac{Mq\tau}{2} - 1 \right)! \left( \frac{q\tau}{2} - 1 \right)!} \left( \frac{\varpi \left( \frac{q\tau}{2}, \frac{z}{2M} \right)}{\left( \frac{q\tau}{2} - 1 \right)!} \right)^{(S-M)} dz, \quad (12) \end{aligned}$$

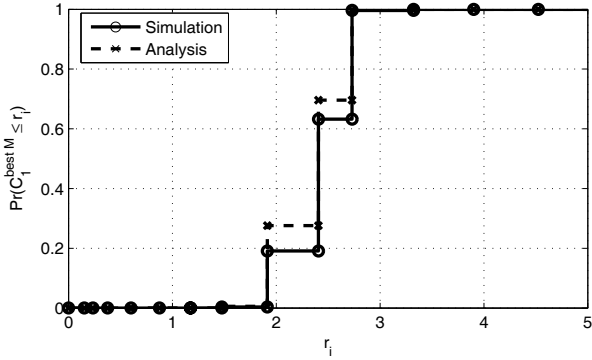


Fig. 2. Plot of the approximate CDF of  $C_1^{\text{bestM}}$  and the CDF generated from simulations ( $S = 6$ ,  $M = 3$ , and  $\sigma_1^2 = 6$  dB).

and  $\beta \approx \sum_{i=1}^U w_i \frac{\alpha_i \frac{Mq\tau}{2} - 1}{(\frac{Mq\tau}{2} - 1)!} \left( \frac{\varpi(\frac{q\tau}{2}, \frac{\alpha_i}{M})}{(\frac{q\tau}{2} - 1)!} \right)^{(S-M)}$ . Here,  $w_i$  and  $\alpha_i$  are the Gauss-Laguerre weights and abscissas, respectively, and are tabulated in [32, Tbl. 25.9].

*Proof:* The proof is relegated to Appendix B. ■

For numerical accuracy,  $U = 6$  suffices. In Figure 2, we compare for SISO the cumulative density function (CDF) of CQI given in (12) and the empirical CDF generated using 50,000 samples for  $\sigma_1^2 = 6$  dB. The set of rates  $\{r_1, \dots, r_{16}\}$  for the  $L = 16$  different MCSs used in LTE are as per [2, Tbl. 10.1]. We can see that the approximation error is always less than 10%. A similar behavior is observed for other values of  $\sigma_1^2$  also. Notice that the probability that the user reports low rate MCSs ( $r_i \leq 1.91$  bits/symbol) or very high rate MCSs ( $r_i \geq 2.73$  bits/symbol) is negligible in this example.

**Claim 3:** For the PF scheduler, the probability that UE  $k$  is selected (sel.) for PRB  $n$  given that  $k \in \mathcal{Z}$  and  $C_k^{\text{bestM}} = r_i$  is

$$\Pr(k \text{ is sel. for } n^{\text{th}} \text{ PRB} | k \in \mathcal{Z}, C_k^{\text{bestM}} = r_i) = \prod_{\substack{l \in \mathcal{Z} \\ l \neq k}} \Pr(C_l^{\text{bestM}} \leq \vartheta_{l,i}), \quad (13)$$

where  $\vartheta_{l,i}$  is the largest rate that is strictly less than  $\frac{E[C_l^{\text{bestM}}]}{E[C_k^{\text{bestM}}]} r_i$  and  $\Pr(C_l^{\text{bestM}} \leq \vartheta_{l,i})$  is given by Claim 2.

*Proof:* The result follows because UE  $k$ , which reports a CQI of  $r_i$ , is selected only if  $C_l^{\text{bestM}} < \frac{E[C_l^{\text{bestM}}]}{E[C_k^{\text{bestM}}]} r_i$ , for all UEs  $l \neq k$ .<sup>5</sup> ■

Similarly, for the greedy scheduler, we have the following result.

**Claim 4:** For the greedy scheduler, the probability that UE  $k$  is selected for PRB  $n$  given that  $k \in \mathcal{Z}$  and  $C_k^{\text{bestM}} = r_i$  is

$$\Pr(k \text{ is sel. for } n^{\text{th}} \text{ PRB} | k \in \mathcal{Z}, C_k^{\text{bestM}} = r_i) = \sum_{\mathcal{A} \subseteq \mathcal{Z} \setminus \{k\}} \frac{1}{|\mathcal{A}| + 1} \left[ \prod_{t_1 \in \mathcal{A}} \Pr(C_{t_1}^{\text{bestM}} = r_i) \right]$$

<sup>5</sup>The equality case  $C_l^{\text{bestM}} = \frac{E[C_l^{\text{bestM}}]}{E[C_k^{\text{bestM}}]} r_i$  occurs with probability zero in a random deployment of users in a cell, and is, therefore, not considered.

$$\times \left[ \prod_{t_2 \in \mathcal{Z} \setminus (\mathcal{A} \cup \{k\})} \Pr(C_{t_2}^{\text{bestM}} \leq r_{i-1}) \right], \quad (14)$$

where  $\sum_{\mathcal{A} \subseteq \mathcal{Z} \setminus \{k\}}$  denotes the summation over all subsets  $\mathcal{A}$  of  $\mathcal{Z} \setminus \{k\}$ .

*Proof:* Given that  $C_k^{\text{bestM}} = r_i$ , if  $|\mathcal{A}|$  other UEs from the set  $\mathcal{Z}$  also report the same highest CQI, then UE  $k$  is selected with probability  $1/(|\mathcal{A}| + 1)$ . Hence, the result follows. ■

We now derive a general expression for the throughput per PRB of the UE selected subband feedback scheme as a function of the scheduler, multiple antenna mode, and other system parameters.

**Result 1:** The average throughput,  $\bar{R}$ , for PRB  $n$ , is

$$\begin{aligned} \bar{R} &= \sum_{\mathcal{Z}} \Pr(\mathcal{Z}) \sum_{k \in \mathcal{Z}} \sum_{i=1}^L r_i \Pr(C_k^{\text{bestM}} = r_i) \\ &\times (1 - \Pr(\gamma_{n,k} < T_{i-1} | C_k^{\text{bestM}} = r_i, k \text{ is sel. for } n^{\text{th}} \text{ PRB})) \\ &\times \Pr(k \text{ is sel. for } n^{\text{th}} \text{ PRB} | k \in \mathcal{Z}, C_k^{\text{bestM}} = r_i), \quad (15) \end{aligned}$$

where  $\Pr(\gamma_{n,k} < T_{i-1} | C_k^{\text{bestM}} = r_i, k \text{ is sel. for } n^{\text{th}} \text{ PRB})$  is given in Claim 1 and  $\Pr(C_k^{\text{bestM}} = r_i)$  is given in Claim 2.  $\Pr(k \text{ is sel. for } n^{\text{th}} \text{ PRB} | k \in \mathcal{Z}, C_k^{\text{bestM}} = r_i)$  is given by Claims 3 and 4 for the PF and greedy schedulers, respectively. Also,  $\Pr(\mathcal{Z}) = (\frac{M}{S})^{|\mathcal{Z}|} (1 - \frac{M}{S})^{K - |\mathcal{Z}|}$ .

*Proof:* Since the SNRs of different PRBs of a user are i.i.d., the probability that a user selects the subband  $s$  is  $\frac{M}{S}$ . Hence,  $\Pr(\mathcal{Z}) = (\frac{M}{S})^{|\mathcal{Z}|} (1 - \frac{M}{S})^{K - |\mathcal{Z}|}$ . A rate  $r_i$  is achieved if the user selected for the PRB fed back a CQI value equal to  $r_i$  and there was no outage. The law of total expectation then yields (15). ■

### C. Subband-Level CQI Feedback Scheme

We derive expressions for the throughputs of all the three schedulers. The following claims shall lead us to the final expression for the throughput in (18).

**Claim 5:** Let UE  $k$  be selected for the  $n^{\text{th}}$  PRB and the CQI value reported by it be  $r_i$ . The probability of an outage in the  $n^{\text{th}}$  PRB, i.e.,  $\gamma_{n,k} \leq T_{i-1}$ , is

$$\begin{aligned} &\Pr(\gamma_{n,k} < T_{i-1} | C_{s,k}^{\text{sub}} = r_i, k \text{ is sel. for } n^{\text{th}} \text{ PRB}) \\ &= \frac{1}{(\frac{\tau}{2} - 1)!} \sum_{l=0}^{\frac{(q-1)\tau}{2} - 1} \frac{(-1)^l (T_{i-1} - b)^{\frac{\tau}{2} + 1}}{(\frac{\tau}{2} + l)! \left( \frac{(q-1)\tau}{2} - l - 1 \right)! (2a)^{\frac{\tau}{2} + 1}} \\ &\times \frac{1}{\Pr(C_{s,k}^{\text{sub}} = r_i)} \left[ \varpi \left( \frac{(q-1)\tau}{2} - l, \frac{qT_i - (q-1)b}{2a} \right) \right. \\ &\quad \left. - \varpi \left( \frac{(q-1)\tau}{2} - l, \frac{qT_{i-1} - (q-1)b}{2a} \right) \right]. \quad (16) \end{aligned}$$

Here,  $\Pr(C_{s,k}^{\text{sub}} = r_i) = \Pr(C_{s,k}^{\text{sub}} \leq r_i) - \Pr(C_{s,k}^{\text{sub}} \leq r_{i-1})$ , where  $\Pr(C_{s,k}^{\text{sub}} \leq r_i) = \frac{1}{(\frac{q\tau}{2} - 1)!} \varpi \left( \frac{q\tau}{2}, \frac{q}{2a} (T_i - b) \right)$ .

*Proof:* The proof is relegated to Appendix C. ■

We now derive scheduler-specific expressions for the probability that a UE  $k$  is selected for the  $n^{\text{th}}$  PRB given that  $C_{s,k}^{\text{sub}} = r_i$ . For the RR scheduler, it is trivially  $\frac{1}{K}$ .

**Claim 6:** For the PF scheduler, the probability that UE  $k$  is selected for PRB  $n$  given that  $C_{s,k}^{\text{sub}} = r_i$  is

$$\Pr(k \text{ is sel. for } n^{\text{th}} \text{ PRB} | C_{s,k}^{\text{sub}} = r_i) = \prod_{\substack{l=1 \\ l \neq k}}^K \Pr(C_{s,l}^{\text{sub}} \leq \vartheta_{l,i}),$$

where  $\vartheta_{l,i}$  is the largest rate among  $\{r_1, \dots, r_L\}$  that is strictly less than  $\frac{E[C_{s,l}^{\text{sub}}]}{E[C_{s,k}^{\text{sub}}]} r_i$  and  $\Pr(C_{s,l}^{\text{sub}} \leq \vartheta_{l,i})$  is as given in Claim 5.

*Proof:* The result follows because UE  $k$ , which reports a CQI of  $r_i$ , is selected only if  $C_{s,l}^{\text{sub}} < \frac{E[C_{s,l}^{\text{sub}}]}{E[C_{s,k}^{\text{sub}}]} r_i$ , for all  $l \neq k$ . ■

**Claim 7:** For the greedy scheduler, the probability that UE  $k$  is selected for the  $n^{\text{th}}$  PRB given that  $C_{s,k}^{\text{sub}} = r_i$  is

$$\begin{aligned} & \Pr(k \text{ is sel. for } n^{\text{th}} \text{ PRB} | C_{s,k}^{\text{sub}} = r_i) \\ &= \sum_{\mathcal{A} \in \{1, \dots, K\} \setminus \{k\}} \frac{1}{|\mathcal{A}| + 1} \left[ \prod_{t_1 \in \mathcal{A}} \Pr(C_{s,t_1}^{\text{sub}} = r_i) \right] \\ & \quad \times \left[ \prod_{t_2 \in \{1, \dots, K\} \setminus (\mathcal{A} \cup \{k\})} \Pr(C_{s,t_2}^{\text{sub}} \leq r_{i-1}) \right], \quad (17) \end{aligned}$$

where  $\Pr(C_{s,k}^{\text{sub}} = r_i)$  and  $\Pr(C_{s,k}^{\text{sub}} \leq r_i)$  are given in Claim 5, and  $\sum_{\mathcal{A} \in \{1, \dots, K\} \setminus \{k\}}$  denotes the summation over all subsets  $\mathcal{A}$  of  $\{1, \dots, K\} \setminus \{k\}$ .

*Proof:* The greedy scheduler selects a UE  $k$  for the  $n^{\text{th}}$  PRB if  $k = \arg \max_{1 \leq k \leq K} \{C_{s,k}^{\text{sub}}\}$ . Given that  $C_{s,k}^{\text{sub}} = r_i$ , let  $\mathcal{A}$  be the set of other UEs that have also reported  $r_i$  for the subband  $s$ . Then, UE  $k$  is selected with probability  $1/(|\mathcal{A}| + 1)$  if all other UEs from the set  $\{1, \dots, K\} \setminus (\mathcal{A} \cup \{k\})$  have reported a CQI less than or equal to  $r_{i-1}$ . Hence, the above result follows. ■

Using the above claims, we now derive a general expression for the throughput of the subband-level feedback scheme.

**Result 2:** The average throughput,  $\bar{R}$ , for all the three schedulers for PRB  $n$  is

$$\begin{aligned} \bar{R} &= \sum_{k=1}^K \sum_{i=1}^L r_i \Pr(C_{s,k}^{\text{sub}} = r_i) \Pr(k \text{ is sel. for } n^{\text{th}} \text{ PRB} | C_{s,k}^{\text{sub}} = r_i) \\ & \times (1 - \Pr(\gamma_{n,k} < T_{i-1} | C_{s,k}^{\text{sub}} = r_i, k \text{ is sel. for } n^{\text{th}} \text{ PRB})). \quad (18) \end{aligned}$$

$\Pr(\gamma_{n,k} < T_{i-1} | C_{s,k}^{\text{sub}} = r_i, k \text{ is sel. for } n^{\text{th}} \text{ PRB})$  and  $\Pr(C_{s,k}^{\text{sub}} = r_i)$  are given in Claim 5. For the PF and greedy schedulers,  $\Pr(k \text{ is sel. for } n^{\text{th}} \text{ PRB} | C_{s,k}^{\text{sub}} = r_i)$  is given by Claims 6 and 7, respectively, and is equal to  $\frac{1}{K}$  for the RR scheduler.

*Proof:* A rate  $r_i$  is achieved if the UE selected for the PRB fed back a CQI value equal to  $r_i$  and there was no outage. This results in the expression for the average throughput in (18). ■

#### D. Asymptotic Insights For Symmetric Users Scenario

To get more analytical insights into the performance of the CQI feedback schemes, we now consider the special symmetric case, in which all channels are statistically identical, *i.e.*,

$\sigma_k^2 = \sigma^2$ , for  $1 \leq k \leq K$ . In this case, the performance of the greedy and PF schedulers is the same. As proved in Appendix D, we state the following results:

1) As the number of UEs  $K \rightarrow \infty$ ,  $\bar{R}$  tends to  $r_L(1 - p_{\text{out}}(r_L))$  for both UE selected subband feedback and subband-level feedback. Here,  $p_{\text{out}}(r_L)$  is the outage probability, and is given in Claims 1 and 5 for UE selected subband feedback and subband-level feedback, respectively. Thus, the coarse frequency granularity of the feedback prevents the throughput from reaching  $r_L$  even when  $K \rightarrow \infty$ .

2) As  $\sigma^2 \rightarrow \infty$ ,  $\bar{R} \rightarrow r_L(1 - \lim_{\sigma^2 \rightarrow \infty} p_{\text{out}}(r_L))$  and  $\lim_{\sigma^2 \rightarrow \infty} p_{\text{out}}(r_L) = O((\sigma^2)^{-\frac{\alpha}{2}}) \rightarrow 0$ , for both the feedback schemes.

## V. SIMULATION RESULTS AND COMPARISONS

We now verify the analytical results using Monte Carlo simulations that average over 50,000 samples.

### A. Simulation Setup

The set of link adaptation thresholds are generated using the coding gain loss model of [33], [34], in which  $r_i = \log_2(1 + \zeta T_{i-1})$ . A smaller  $\zeta$ , which is also called the coding gain loss, means a lower (tighter) bit error rate constraint [11].

A subband consists of  $q = 4$  PRBs. The number of subbands is  $S = 6$ , which corresponds to  $B = 5$  MHz bandwidth. In UE selected subband feedback, a UE selects  $M = 3$  out of  $S = 6$  subbands. The channel gains of the PRBs for different transmit-receive antenna pairs for UE  $k$  are generated as independent zero-mean complex Gaussian RVs with variance  $\sigma_k^2$  that is given as follows. For the  $K$  users, we set  $\sigma_k^2 = \lambda/\alpha^{k-1}$ ,  $1 \leq k \leq K$ . Note that the mean SNR is proportional to  $\sigma_k^2$ , with the constant of proportionality depending on the multiple antenna mode used. The farther  $\alpha$  is from 1, the more statistically different the users' channels are. This models the scenario where the users are at different distances from the BS. Unless mentioned otherwise,  $\lambda = 10$  dB,  $\alpha = 1.2$ ,  $\zeta = 0.398$  [33], and  $K = 6$ .

Since the throughput for SIMO and closed-loop MISO are the same for a given  $\sigma_k^2$ , results are shown for SIMO only. Given the space constraints, results are shown for a representative subset of combinations of feedback schemes, schedulers, and multiple antenna modes.

### B. General Case: Asymmetric Users

We first study the system throughput for the general case in which the users see statistically different channels. Figure 3 plots the average throughput as a function of  $K$  for the UE selected subband scheme with the PF scheduler for SISO, SIMO ( $N_r = 2$ ), and single-stream MIMO. When  $K > 4$ , the throughput decreases marginally as the number of users increases. This is because the PF scheduler ensures fairness among the users even though the mean SNR of the additional users is lower. A similar effect is observed for the subband-level feedback scheme, as well. We see that the analysis and simulation results differ by no more than 12%. The difference occurs because of the approximation in Claim 2.

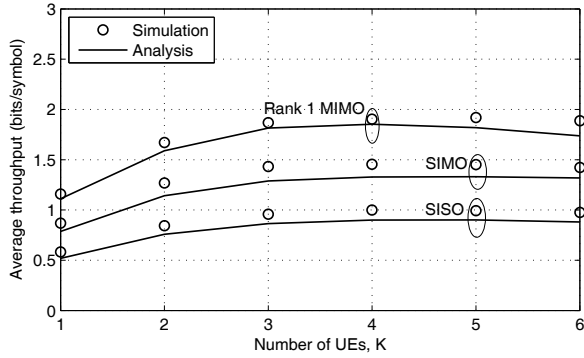


Fig. 3. Average throughput vs. number of users from analysis and simulations for the PF scheduler with UE selected subband feedback.

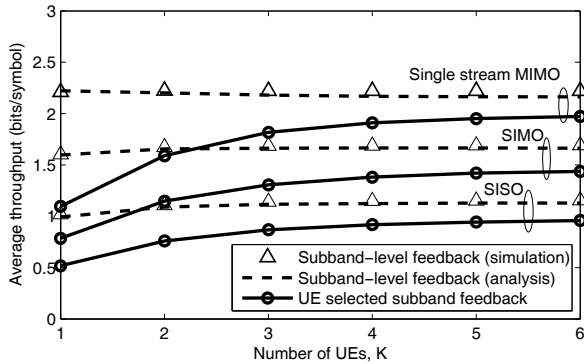


Fig. 4. Average throughput vs. number of users for the greedy scheduler for different multiple antenna modes and CQI feedback schemes.

The throughputs of single-stream MIMO and SIMO are 90% and 45%, respectively, more than SISO.

To compare the two CQI feedback schemes, Figure 4 plots the average throughput for the subband-level and UE selected subband feedback schemes for the greedy scheduler. This is done for SISO, SIMO, and single-stream MIMO. We see that for the subband-level feedback, the analysis and simulation results match very well. The simulation results for the PF scheduler, which have already been plotted in Figure 3, are not repeated here to ensure clarity. As the number of UEs increases, the throughput of the UE selected subband scheme becomes quite close to that of the subband-level feedback scheme for all the multiple antenna modes. Note that as  $K$  increases, the throughput of the subband-level feedback scheme does not increase for the chosen simulation parameters. This is because, for the asymmetric case, each UE that is added sees a progressively weaker channel (on average). Therefore, the performance gains from having more users to choose from decrease faster than one would expect from the law of diminishing returns. We have also found in our analysis and simulations that the outage probability increases marginally as  $K$  increases. The combined effect of these is observed in the figure.

To quantify the effect of asymmetry among users, Figure 5 plots the throughput as a function of  $\alpha$  for the subband-level feedback scheme for SISO. Recall that the farther  $\alpha$  is from 1, the more asymmetric are the users' channels. As

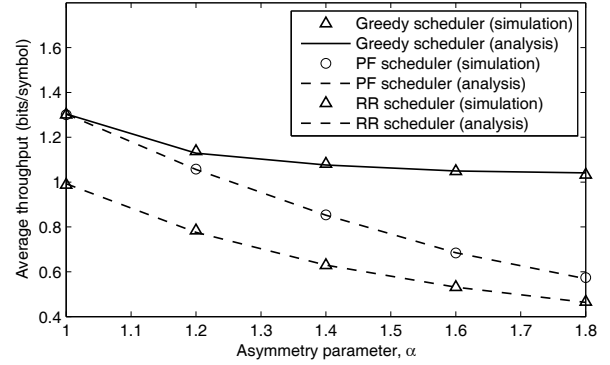


Fig. 5. Average throughput vs. asymmetry parameter,  $\alpha$ , for subband-level feedback for PF, greedy, and RR schedulers.

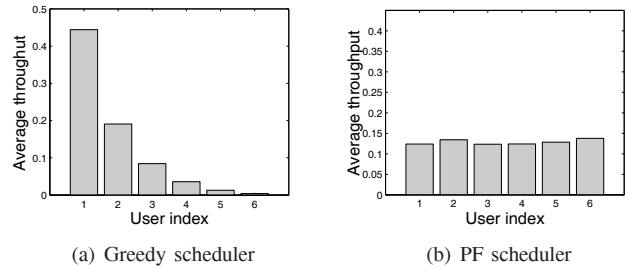


Fig. 6. Comparison of the throughputs of individual UEs for the PF and greedy schedulers for subband-level feedback ( $\alpha = 1.2$  and  $\lambda = 10$  dB).

expected, since both PF and RR schedulers try to ensure fairness among users, the throughput drops as  $\alpha$  increases. In fact, the throughput drops more rapidly for the PF scheduler than the RR scheduler. At  $\alpha = 1$ , both the greedy and PF schedulers give the same throughput since all users have the same mean SNR. For the UE selected subband scheme also, a similar behavior is observed. Figure 6 delves into this aspect further by showing the throughput for each UE. It clearly brings out the fairness achieved by PF. This effect was seen for all the other multiple antenna modes and for the UE selected subband scheme, as well.

Table II gives a comprehensive list of throughputs – from both analysis and simulations – of a combination of different feedback schemes, schedulers, and multiple antenna modes for different numbers of users. For UE selected subband feedback, the difference between analysis and simulation is at most 12%. As mentioned, the difference is due to the approximation used in Claim 2. For single-stream MIMO, the additional approximation in (7) marginally increases the difference. The error is considerably smaller for the subband-level feedback scheme. As expected, for a given set of UEs, the greedy scheduler always yields a higher throughput. For larger bandwidths, the throughput of UE selected subband feedback will improve due to increased frequency diversity, but that of the subband-level feedback scheme will remain the same.

### C. Effect of Correlation Across Space and Frequency

For channels with small delay spreads, the assumption that different PRBs experience independent fading may not

Greedy Scheduler			
SISO			
No. of UEs ( $K$ )	2	4	6
UE selected subband	0.76 (0.84)	0.92 (1.02)	0.96 (1.06)
Subband-level	1.09 (1.09)	1.12 (1.12)	1.13 (1.13)
SIMO			
UE selected subband	1.15 (1.26)	1.38 (1.54)	1.43 (1.59)
Subband-level	1.66 (1.66)	1.66 (1.67)	1.66 (1.67)
Single stream MIMO			
UE selected subband	1.59 (1.69)	1.91 (2.07)	1.97 (2.15)
Subband-level	2.18 (2.23)	2.18 (2.22)	2.18 (2.22)
Open-loop MISO			
UE selected subband	0.83 (0.90)	1.00 (1.10)	1.04 (1.14)
Subband-level	1.18 (1.18)	1.19 (1.19)	1.20 (1.20)
PF Scheduler			
SISO			
No. of UEs ( $K$ )	2	4	6
UE selected subband	0.84 (0.76)	0.90 (0.99)	0.88 (0.97)
Subband-level	1.09 (1.09)	1.10 (1.11)	1.05 (1.05)
SIMO			
UE selected subband	1.14 (1.26)	1.33 (1.45)	1.32 (1.40)
Subband-level	1.65 (1.65)	1.59 (1.59)	1.49 (1.49)
Single stream MIMO			
UE selected subband	1.59 (1.67)	1.85 (1.91)	1.76 (1.82)
Subband-level	2.18 (2.19)	2.07 (2.09)	1.91 (1.94)
Open-loop MISO			
UE selected subband	0.83 (0.90)	0.96 (1.05)	0.92 (1.01)
Subband-level	1.18 (1.18)	1.16 (1.16)	1.09 (1.09)

TABLE II

COMPARISON OF THROUGHPUT (IN BITS/SYMBOL) ACROSS CQI FEEDBACK SCHEMES, SCHEDULERS, AND MULTIPLE ANTENNA MODES. ANALYSIS RESULTS ARE SHOWN WITHOUT BRACKETS AND SIMULATION RESULTS ARE SHOWN WITHIN BRACKETS.

be accurate. To understand the effect of this correlation, we simulate a geometrically decaying correlation model in which  $\frac{E[h_{n,k}(i,j)h_{m,k}^*(i,j)]}{\sigma_k^2} = \rho_f^{|n-m|}$ , for all PRBs  $n$  and  $m$  as has also been done in [12]. Figure 7 plots the throughput of subband-level feedback scheme for different values of  $\rho_f$  for the greedy scheduler. It clearly shows that unless the PRBs are highly correlated, the throughput does not increase significantly. In order to further understand the effect of correlation across PRBs, we also plot the throughput for the Typical Urban (TU) and Pedestrian B (PedB) standardized channel models, which are often used in LTE contributions [26], [27] and papers [23], [35]. Since the coherence bandwidths of these channels is much more than 180 kHz, the PRB SNRs, which are used in our model, are generated by simply taking an arithmetic average of the SNRs of the constituent subcarriers.

Figure 8 quantifies the effect of spatial correlation. It plots the throughput of the subband-level feedback scheme for the greedy scheduler with SIMO and  $\rho_f = 0$ . Antenna correlation is modeled using the widely used Kronecker model [36], with the correlation between the two antennas given by  $\rho_s$ . We observe that as  $\rho_s$  increases, the throughput decreases due to the reduction in the effective diversity. However, spatial correlation has a marginal impact on the throughput. The figure also plots the throughput of the Urban Macrocell: Non Line-of-Sight (UMa: NLoS) clustered delay line (CDL) model that is specified in the M.2135 report [37, Tbl. A1-15], which provides guidelines for evaluation of radio interface technologies for International Mobile Telecommunications-Advanced (IMT-

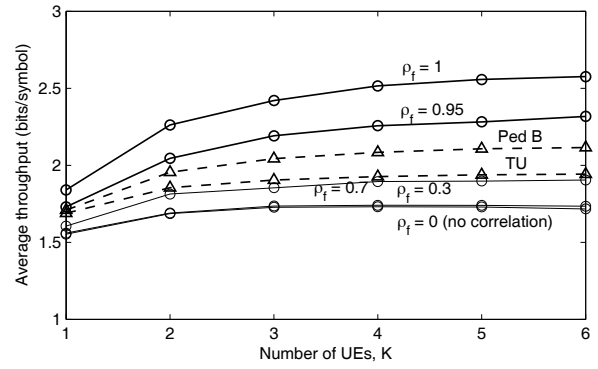


Fig. 7. Effect of correlation in frequency for subband-level feedback with greedy scheduler. Also shown are results for Typical Urban and Pedestrian B frequency-selective channel models. All results except  $\rho_f = 0$  are from simulations.

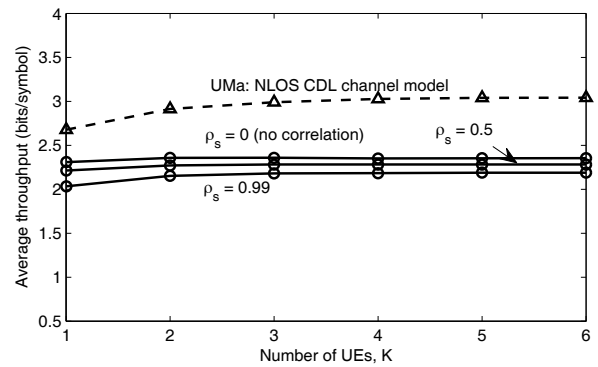


Fig. 8. Effect of correlation in space for subband-level feedback with greedy scheduler. Also shown are results for the UMa: NLoS channel model.

Advanced). In this channel model, both frequency and spatial correlations are present. While spatial correlation marginally reduces the throughput, correlation in frequency increases the throughput. The net result is an increase in throughput compared to the uncorrelated space and frequency case analyzed in this paper.

#### D. Symmetric Users Scenario

We now study the symmetric users scenario ( $\alpha = 1$  and  $\sigma_k^2 = \sigma^2$ ) to gain further insights into the system behavior. Figure 9 plots the average throughput for different values of  $M$ , for SIMO, PF scheduler, and  $K = 6$ . As  $q$  increases from 2 to 4, the throughput decreases. This is because the outage probability increases since the CQI fed back is averaged over more subbands. As  $M$  increases, the throughput initially increases and reaches a maximum at  $M = 3$  for both  $q = 2$  and 4. This is because the odds that any given subband is reported as one of the best  $M$  subbands of at least one UE increase as  $M$  increases. However, beyond  $M = 3$ , the throughput decreases because each UE feeds back only one CQI that is averaged over more subbands. This increase in the coarseness in the frequency granularity of feedback increases the outage probability. Note that the system designer may still choose a value of  $M$  less than 3 depending on how limited the uplink feedback bandwidth is. The same effect also occurs

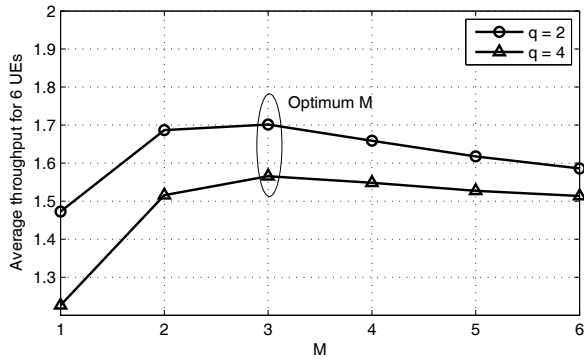


Fig. 9. Average throughput for different values of  $M$  for the PF scheduler with UE selected subband feedback ( $S = 6$  and  $K = 6$ ).

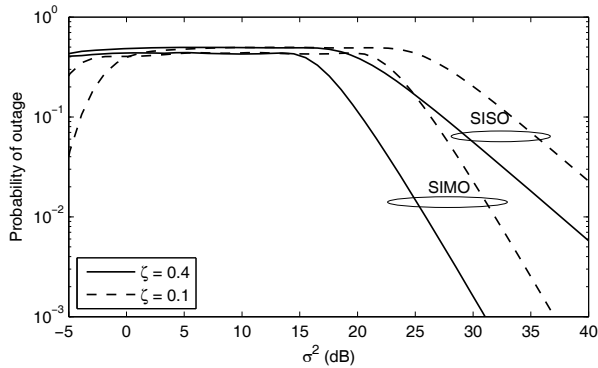


Fig. 10. Comparison of probability of outage as a function of  $\sigma^2$  for different sets of thresholds for subband-level feedback ( $K = 6$  and symmetric users).

for other multiple antenna modes. For the greedy scheduler, the optimum value of  $M$  changes to 4.

Figure 10 studies the effect of the choice of link adaptation thresholds. It plots the outage probability for the subband-level feedback scheme as a function of  $\sigma^2$  for SISO and SIMO. The thresholds  $T_0, \dots, T_L$  are changed by varying  $\zeta$ . We notice that a lower value of  $\zeta$  results in a higher probability of outage for large  $\sigma^2$ . This is because, for large  $\sigma^2$ , the highest rate MCS (rate  $r_L$ ) is chosen most often. The outage probability increases because  $T_{L-1}$  increases as  $\zeta$  decreases. We also observe the probability of outage decreases as  $O(\sigma^{-\tau})$  for large  $\sigma^2$ , as proved in Sec. IV-D. Notice that the outage probability can be significant. The use of EESM instead of the arithmetic mean will reduce the outage probability. Further, as done in [38], the outage probability can be reduced by scaling the average subband SNR by a factor  $\Delta > 1$ .

## VI. CONCLUSIONS

In an OFDMA-based system such as LTE, the frequency-domain scheduler exploits multi-user and frequency diversity by assigning different PRBs to different UEs based on the channel quality information reported by the UEs. The scheduler determines which resource block to allocate to which UE and at what rate to transmit on the basis of the CQI feedback from the UEs. It makes its decisions based on a coarser subband-level feedback that is averaged over multiple

resource blocks. This is true for both the subband-level and UE selected subband CQI feedback schemes, and is done in order to consume less uplink bandwidth.

In this paper, we developed an analytically tractable model for the operation of the CQI feedback schemes of LTE, and analyzed their performance. Our analysis handled a wide range of schedulers – PF, greedy, and RR, and also different multi-antenna diversity modes – SISO, SIMO, open-loop and closed-loop MISO, and single-stream MIMO. The analysis quantified several insights about the joint performance of the feedback schemes with different schedulers and multiple antenna modes, which had hitherto been understood only qualitatively. For example, it showed quantitatively how the performance of the UE selected subband feedback scheme approaches that of the subband-level feedback scheme, and how multiple antenna diversity enhances overall system throughput.

We saw that the coarser frequency-domain feedback can lead to an incorrect MCS being used for some resource blocks, which can result in outage. This outage persists even when the number of users increases asymptotically. The choice of the link adaptation thresholds affects this outage probability. While the paper focused on deriving closed-form expressions for the throughput, the analysis can be also easily extended to derive the CDF of the UE throughput, which is also used in practice to understand system behavior in greater detail.

Note that the analysis does not obviate the need for detailed system-level simulations given the modeling simplifications it uses. However, it is valuable as it provides an independent and common theoretical reference to an LTE system designer, and helps verify large system simulators. It also enables the designer to quickly optimize parameters as a function of the CQI feedback scheme, scheduler, and multiple antenna mode, and save some simulation effort. More generally, it helps us understand how the several techniques proposed and analyzed in isolation and under idealized models in the literature perform together under the constraints imposed by a practical system design.

Generalizing the analysis to include additional radio resource management aspects of LTE and incorporating correlation in frequency and space are interesting problems for future work.

## APPENDIX

### A. Proof of Claim 1

Given that UE  $k$  is selected for the  $n^{\text{th}}$  PRB and  $C_k^{\text{bestM}} = r_i$ , we have

$$\begin{aligned} \psi_k &\triangleq \Pr(\gamma_{n,k} < T_{i-1} | C_k^{\text{bestM}} = r_i, k \text{ is sel. for } n^{\text{th}} \text{ PRB}), \\ &\stackrel{(a)}{=} \Pr(\gamma_{n,k} < T_{i-1} | C_k^{\text{bestM}} = r_i), \\ &= \frac{\Pr(\gamma_{n,k} < T_{i-1}, T_{i-1} \leq \frac{1}{M} \sum_{v \in \mathcal{I}_k} \gamma_{v,k}^{\text{sub}} < T_i)}{\Pr(T_{i-1} \leq \frac{1}{M} \sum_{v \in \mathcal{I}_k} \gamma_{v,k}^{\text{sub}} < T_i)}, \quad (19) \end{aligned}$$

where the set  $\mathcal{I}_k$  must contain the subband  $s$ . Here, (a) follows because the probability of  $\gamma_{n,k} < T_{i-1}$ , given that  $C_k^{\text{bestM}} = r_i$ , does not depend on whether  $k$  is selected for the  $n^{\text{th}}$  PRB.

Without loss of generality, since the PRB SNRs are i.i.d. and so are the subband effective SNRs, let  $n = 1$ ,  $s(1) = 1$ , and  $\mathcal{I}_k = \{1, \dots, M\}$ . Since  $\binom{S-1}{M-1}$  sets of  $M$  subbands contain subband 1, the numerator of (19) is  $\binom{S-1}{M-1} \Pr(\gamma_{1,k} < T_{i-1}, T_{i-1} \leq \sum_{v=1}^M \frac{\gamma_{v,k}^{\text{sub}}}{M} < T_i, \mathcal{I}_k = \{1, \dots, M\})$ . Similarly, the denominator of (19) is given by  $\binom{S-1}{M-1} \Pr(T_{i-1} \leq \frac{1}{M} \sum_{v=1}^M \gamma_{v,k}^{\text{sub}} < T_i, \mathcal{I}_k = \{1, \dots, M\})$ . Substituting these in (19) and using Baye's rule yields

$$\psi_k = \frac{\Pr(\gamma_{1,k} < T_{i-1}, T_{i-1} \leq \frac{1}{M} \sum_{v=1}^M \gamma_{v,k}^{\text{sub}} < T_i)}{\Pr(T_{i-1} \leq \frac{1}{M} \sum_{v=1}^M \gamma_{v,k}^{\text{sub}} < T_i)} \times \frac{\Pr(\mathcal{I}_k = \{1, \dots, M\} | \gamma_{1,k} < T_{i-1}, T_{i-1} \leq \sum_{v=1}^M \frac{\gamma_{v,k}^{\text{sub}}}{M} < T_i)}{\Pr(\mathcal{I}_k = \{1, \dots, M\} | T_{i-1} \leq \frac{1}{M} \sum_{v=1}^M \gamma_{v,k}^{\text{sub}} < T_i)}.$$

Notice that  $Mq - 1$  other PRBs also affect  $\mathcal{I}_k$  in addition to PRB 1. Thus, the event  $\mathcal{I}_k = \{1, \dots, M\}$  depends weakly on the event  $\gamma_{1,k} < T_{i-1}$ . Neglecting the conditioning on  $\gamma_{1,k} < T_{i-1}$  in the numerator and simplifying gives

$$\psi_k \approx \frac{\Pr(\gamma_{1,k} < T_{i-1}, T_{i-1} \leq \frac{1}{M} \sum_{v=1}^M \gamma_{v,k}^{\text{sub}} < T_i)}{\Pr(T_{i-1} \leq \frac{1}{M} \sum_{v=1}^M \gamma_{v,k}^{\text{sub}} < T_i)}. \quad (20)$$

If  $\gamma_{1,k} = y$ , then, from (1) and (8), we have  $\frac{1}{M} \sum_{v=1}^M \gamma_{v,k}^{\text{sub}} = \frac{a}{Mq} R + \frac{(Mq-1)b}{Mq} + \frac{y}{Mq}$ , where  $R$  is a chi-square RV with  $(Mq - 1)\tau$  degrees of freedom and mean  $(Mq - 1)\tau$ . Thus, the numerator in (20) becomes

$$\begin{aligned} & \Pr\left(T_{i-1} \leq \frac{1}{M} \sum_{v=1}^M \gamma_{v,k}^{\text{sub}} < T_i, \gamma_{n,k} < T_{i-1}\right) \\ &= \int_{-b}^{T_{i-1}-b} \frac{y^{\frac{\tau}{2}-1} e^{-\frac{y}{2a}}}{(2a)^{\frac{\tau}{2}} (\frac{\tau}{2} - 1)!} \\ & \times \int_{T_{i-1} - \frac{(Mq-1)b}{Mq} - \frac{y}{Mq}}^{T_i - \frac{(Mq-1)b}{Mq} - \frac{y}{Mq}} \frac{\left(\frac{Mq}{2a}\right)^{\frac{(Mq-1)\tau}{2}} x^{\frac{(Mq-1)\tau}{2}-1} e^{-\frac{Mqx}{2a}}}{\left(\frac{(Mq-1)\tau}{2} - 1\right)!} dx dy. \end{aligned} \quad (21)$$

Using the substitution  $z = x + \frac{y}{Mq}$  and the binomial expansion of  $\left(z - \frac{y}{Mq}\right)^{\frac{(Mq-1)\tau}{2}-1}$ , the integrals can be evaluated in closed-form. Similarly, the denominator in (20) can be simplified to

$$\begin{aligned} & \Pr\left(T_{i-1} \leq \frac{1}{M} \sum_{v=1}^M \gamma_{v,k}^{\text{sub}} < T_i\right) \\ &= \frac{\varpi\left(\frac{Mq\tau}{2}, \frac{Mq}{2a}(T_i - b)\right) - \varpi\left(\frac{Mq\tau}{2}, \frac{Mq}{2a}(T_{i-1} - b)\right)}{\left(\frac{Mq\tau}{2} - 1\right)!}. \end{aligned} \quad (22)$$

Substituting the above results in (20) yields the desired result.

### B. Proof of Claim 2

From Sec. III-A, we know that  $\Pr(C_k^{\text{bestM}} \leq r_i) = \Pr\left(0 \leq \frac{1}{M} \sum_{i=1}^M \gamma_{(i),k}^{\text{sub}} < T_i\right)$ . To evaluate this probability, we

need the PDF of the sum of  $M$  ordered chi-square RVs, which is analytically intractable. For example, in [39], it was computed by numerically inverting the characteristic function of the sum.

The approach below derives a new approximate expression that involves only a single integral.

$$\begin{aligned} & \Pr\left(0 \leq \frac{1}{M} \sum_{i=1}^M \gamma_{(i),k}^{\text{sub}} < T_i\right) \\ & \stackrel{(a)}{=} \sum_{i_1, \dots, i_M} \Pr\left(0 \leq \frac{1}{M} \sum_{i \in \{i_1, \dots, i_M\}} \gamma_{i,k}^{\text{sub}} < T_i, \mathcal{I}_k = \{i_1, \dots, i_M\}\right), \\ & \stackrel{(b)}{=} \binom{S}{M} \Pr\left(0 \leq \frac{1}{M} \sum_{i=1}^M \gamma_{i,k}^{\text{sub}} < T_i, \mathcal{I}_k = \{1, \dots, M\}\right). \end{aligned} \quad (23)$$

Here, (a) follows from the law of total probability. Since the subband SNRs are i.i.d. for a given user and there are  $\binom{S}{M}$  possible combinations of best  $M$  subbands, we get (b), which corresponds to the event  $\Lambda$  that subbands  $1, \dots, M$  are the  $M$  best subbands. Then,

$$\Pr(\Lambda) = \Pr(\gamma_{M+1,k}^{\text{sub}} \leq \min(\gamma_{1,k}^{\text{sub}}, \dots, \gamma_{M,k}^{\text{sub}}), \dots, \gamma_{S,k}^{\text{sub}} \leq \min(\gamma_{1,k}^{\text{sub}}, \dots, \gamma_{M,k}^{\text{sub}})).$$

Since  $\min(\gamma_{1,k}^{\text{sub}}, \dots, \gamma_{M,k}^{\text{sub}}) \leq \frac{1}{M} \sum_{i=1}^M \gamma_{i,k}^{\text{sub}}$ , we get

$$\Pr(\Lambda) \leq \Pr\left(\gamma_{M+1,k}^{\text{sub}} \leq \frac{1}{M} \sum_{i=1}^M \gamma_{i,k}^{\text{sub}}, \dots, \gamma_{S,k}^{\text{sub}} \leq \frac{1}{M} \sum_{i=1}^M \gamma_{i,k}^{\text{sub}}\right).$$

Thus, we get the following upper bound on  $\Pr(C_k^{\text{bestM}} \leq r_i)$ :

$$\begin{aligned} & \Pr(C_k^{\text{bestM}} \leq r_i) \leq \binom{S}{M} \Pr\left(0 \leq \frac{1}{M} \sum_{i=1}^M \gamma_{i,k}^{\text{sub}} < T_i, \right. \\ & \left. \gamma_{M+1,k}^{\text{sub}} \leq \frac{1}{M} \sum_{i=1}^M \gamma_{i,k}^{\text{sub}}, \dots, \gamma_{S,k}^{\text{sub}} \leq \frac{1}{M} \sum_{i=1}^M \gamma_{i,k}^{\text{sub}}\right). \end{aligned}$$

Hence,

$$\begin{aligned} & \Pr(C_k^{\text{bestM}} \leq r_i) \leq \\ & \binom{S}{M} \int_0^{T_i} \Pr\left(\frac{1}{M} \sum_{i=1}^M \gamma_{i,k}^{\text{sub}} = z\right) \Pr(\gamma_{M+1,k}^{\text{sub}} \leq z)^{(S-M)} dz. \end{aligned} \quad (24)$$

At the same time, we know that  $\Pr(C_k^{\text{bestM}} \leq r_L) = 1$ . This motivates the following approximation, which, by design, is exact for  $i = L$ . In it, the upper bound in (24) is divided by a factor  $\binom{S}{M} \beta$ , where

$$\beta = \int_0^{\frac{Mq}{a}(T_L - b)} \frac{z^{\frac{Mq\tau}{2}-1} e^{-\frac{z}{2}}}{2^{\frac{Mq\tau}{2}} \left(\frac{Mq\tau}{2} - 1\right)! \left(\frac{q\tau}{2} - 1\right)!} \left(\frac{\varpi\left(\frac{q\tau}{2}, \frac{z}{2M}\right)}{\left(\frac{q\tau}{2} - 1\right)!}\right)^{(S-M)} dz. \quad (25)$$

This expression is obtained by using (22) and the fact that  $\gamma_{i,k}^{\text{sub}}$  is a chi-square RV with  $2q$  degrees of freedom and mean  $\sigma_k^2$ . The expression for  $\beta$  given in the claim is a Gauss-Laguerre quadrature approximation [32, Tbl. 25.9] of (25).

### C. Proof of Claim 5

Since the event that  $C_{s,k}^{\text{sub}} \leq r_i$  is same as the event  $\gamma_{s,k}^{\text{sub}} \leq T_i$ , we have

$$\Pr(C_{s,k}^{\text{sub}} \leq r_i) = \Pr(\gamma_{s,k}^{\text{sub}} \leq T_i) = \int_0^{\frac{a}{2}(T_i-b)} \frac{x^{\frac{q\tau}{2}-1} e^{-\frac{x}{2a}}}{2^{\frac{q\tau}{2}-1} (\frac{q\tau}{2}-1)!} dx. \quad (26)$$

The expression in Claim 5 for  $\Pr(C_{s,k}^{\text{sub}} \leq r_i)$  then follows from the definition of the Incomplete Gamma function. Given that UE  $k$  is selected for the  $n^{\text{th}}$  PRB and  $C_{s,k}^{\text{sub}} = r_i$ , we have

$$\Pr(\gamma_{n,k} < T_{i-1} | C_{s,k}^{\text{sub}} = r_i, k \text{ is sel. for } n^{\text{th}} \text{ PRB}) \quad (27)$$

$$\begin{aligned} &\stackrel{(a)}{=} \Pr(\gamma_{n,k} < T_{i-1} | C_{s,k}^{\text{sub}} = r_i), \\ &= \frac{\Pr(T_{i-1} \leq \gamma_{s,k}^{\text{sub}} < T_i, \gamma_{n,k} < T_{i-1})}{\Pr(C_{s,k}^{\text{sub}} = r_i)}. \end{aligned} \quad (28)$$

As in Appendix A, (a) follows because the probability of  $\gamma_{n,k} < T_{i-1}$ , given that  $C_{s,k}^{\text{sub}} = r_i$ , does not depend on whether  $k$  is selected for the  $n^{\text{th}}$  PRB.

If  $\gamma_{n,k} = y$ , then  $\gamma_{s,k}^{\text{sub}} = \frac{a}{q}R + \frac{(q-1)b}{q} + \frac{y}{q}$ , where  $R$  is a chi-square RV with  $(q-1)\tau$  degrees of freedom and mean  $(q-1)\tau$ . Consequently, the numerator in (27) is evaluated as follows:

$$\begin{aligned} \Pr(T_{i-1} \leq \gamma_{s,k}^{\text{sub}} < T_i, \gamma_{n,k} < T_{i-1}) &= \int_{-b}^{T_{i-1}-b} \frac{y^{\frac{\tau}{2}-1} e^{-\frac{y}{2a}}}{(2a)^{\frac{\tau}{2}} (\frac{\tau}{2}-1)!} \\ &\times \int_{T_{i-1}-\frac{(q-1)b}{q}-\frac{y}{q}}^{T_i-\frac{(q-1)b}{q}-\frac{y}{q}} \frac{(\frac{q}{2a})^{\frac{(q-1)\tau}{2}} x^{\frac{(q-1)\tau}{2}-1} e^{-\frac{qx}{2a}}}{((\frac{q-1)\tau}{2}-1)!} dx dy. \end{aligned} \quad (29)$$

By substituting  $z = x + \frac{y}{q}$  and using binomial expansion of  $(z - \frac{y}{q})^{\frac{(q-1)\tau}{2}-1}$ , the above integrals can be evaluated in closed-form. Substituting it in (27) along with results from Claim 5 yields the desired result.

### D. Asymptotic Results for Symmetric Users Scenario

1)  $K \rightarrow \infty$ : For the symmetric scenario, the average throughput expression in (15) for UE selected subband feedback reduces to

$$\begin{aligned} \bar{R} &= \sum_{i=1}^L r_i (1 - p_{\text{out}}(r_i)) \sum_{k=0}^K \binom{K}{k} \left(\frac{M}{S}\right)^k \\ &\times \left(1 - \frac{M}{S}\right)^{K-k} \left(\Pr(C_1^{\text{bestM}} \leq r_i)^k - \Pr(C_1^{\text{bestM}} \leq r_{i-1})^k\right). \end{aligned} \quad (30)$$

As  $K \rightarrow \infty$ ,  $\sum_{k=0}^K \binom{K}{k} \left(\frac{M}{S}\right)^k \Pr(C_1^{\text{bestM}} \leq r_i)^k \left(1 - \frac{M}{S}\right)^{K-k} \rightarrow \left(1 - \frac{M}{S}\right)^K \Pr(C_1^{\text{bestM}} \leq r_i)^K$ . Consequently, for all  $1 \leq i < L$ ,  $\left(1 - \frac{M}{S}\right)^K \Pr(C_1^{\text{bestM}} \leq r_i)^K \rightarrow 0$ . When  $i = L$ , the above expression tends to 1. Hence, the result follows.

The corresponding average throughput expression for subband-level feedback in (18) reduces to

$$\bar{R} = \sum_{i=1}^L r_i (1 - p_{\text{out}}(r_i)) \left[ \Pr(C_{s,1}^{\text{sub}} \leq r_i)^K - \Pr(C_{s,1}^{\text{sub}} \leq r_{i-1})^K \right].$$

Clearly, as  $K \rightarrow \infty$ ,  $\bar{R} \rightarrow r_L (1 - p_{\text{out}}(r_L))$ , since  $\Pr(C_{s,1}^{\text{sub}} \leq r_i) < 1$ , for  $1 \leq i < L$ , and  $\Pr(C_{s,1}^{\text{sub}} \leq r_L) = 1$ .

2)  $\sigma^2 \rightarrow \infty$ : For UE selected subband feedback, from (23), we get

$$\begin{aligned} \Pr(C_1^{\text{bestM}} \leq r_i) &= \binom{S}{M} \Pr\left(0 \leq \frac{1}{M} \sum_{i=1}^M \gamma_{i,1}^{\text{sub}} < T_i\right) \\ &\times \Pr\left(\mathcal{I}_k = \{1, \dots, M\} \mid 0 \leq \frac{1}{M} \sum_{i=1}^M \gamma_{i,1}^{\text{sub}} < T_i\right). \end{aligned} \quad (31)$$

As  $\sigma^2 \rightarrow \infty$ ,  $a \rightarrow \infty$  and  $b \leq 0$  always (as can be seen from Table I). Hence, from (22), it follows that as  $\sigma^2 \rightarrow \infty$ ,  $\Pr\left(0 \leq \frac{1}{M} \sum_{i=1}^M \gamma_{i,1}^{\text{sub}} < T_i\right) \rightarrow 0$ , for  $1 \leq i < L$ , and  $\Pr(C_1^{\text{bestM}} \leq r_L) = 1$ . It then follows from (30) that

$$\bar{R} \rightarrow r_L \left(1 - \lim_{\sigma^2 \rightarrow \infty} p_{\text{out}}(r_L)\right),$$

where  $p_{\text{out}}(r_L)$  is given by (10).

Taking the limit  $\sigma^2 \rightarrow \infty$  in (10) yields

$$\begin{aligned} \lim_{\sigma^2 \rightarrow \infty} p_{\text{out}}(r_L) &= \lim_{\sigma^2 \rightarrow \infty} \frac{\left(\frac{Mq\tau}{2} - 1\right)!}{\left(\frac{\tau}{2} - 1\right)!} \\ &\times \sum_{l=0}^{\frac{Mq-1}{2}\tau-1} \frac{(-1)^l (T_{L-1} - b)^{\frac{\tau}{2}+l}}{\left(\frac{\tau}{2} + l\right)! \left(\frac{Mq-1}{2}\tau - l - 1\right)! (2a)^{\frac{\tau}{2}+l}}. \end{aligned} \quad (32)$$

Here, we used the result that as  $u \rightarrow \infty$ ,  $\varpi(p, u) \rightarrow \frac{1}{p} e^{-u} u^p$ . Using the inequality  $\frac{\tau}{2} \leq \frac{\tau}{2} + l \leq (Mq-1)\frac{\tau}{2} - 1$ , we can sandwich (32) as follows:

$$\begin{aligned} \lim_{\sigma^2 \rightarrow \infty} p_{\text{out}}(r_L) &\leq \frac{\left(\frac{Mq\tau}{2} - 2\right)! \left(\frac{T_{L-1}-b}{2a}\right)^{\frac{\tau}{2}} \left(1 - \frac{T_{L-1}-b}{2a}\right)^{\frac{Mq-1}{2}\tau-1}}{\left(\frac{Mq-1}{2}\tau - 1\right)! \left(\frac{\tau}{2} - 1\right)!} \\ &\leq \lim_{\sigma^2 \rightarrow \infty} p_{\text{out}}(r_L) \leq \\ &\lim_{\sigma^2 \rightarrow \infty} \frac{\left(\frac{Mq\tau}{2} - 1\right)! \left(\frac{T_{L-1}-b}{2a}\right)^{\frac{\tau}{2}} \left(1 - \frac{T_{L-1}-b}{2a}\right)^{\frac{Mq-1}{2}\tau-1}}{\left(\frac{Mq-1}{2}\tau - 1\right)! \frac{\tau}{2}!}. \end{aligned} \quad (33)$$

Thus,  $\lim_{\sigma^2 \rightarrow \infty} p_{\text{out}}(r_L) = O(a^{-\frac{\tau}{2}}) = O((\sigma^2)^{-\frac{\tau}{2}})$ . Hence, the result. Similarly for subband-level feedback, it can be shown that  $\bar{R}$  tends to  $r_L$  as  $\sigma^2 \rightarrow \infty$ .

### REFERENCES

- [1] "Evolved universal terrestrial radio access (E-UTRA); physical channels and modulation (release 8)," Tech. Rep. 36.211 (v8.4.0), 3rd Generation Partnership Project (3GPP), 2008.
- [2] S. Sesia, I. Toufik, and M. Baker, *LTE - The UMTS Long Term Evolution, From Theory to Practice*. John Wiley and Sons, 2009.
- [3] D. Gesbert and M.-S. Alouini, "How much feedback is multiuser diversity really worth?," in *Proc. ICC*, pp. 234-238, Jul. 2004.
- [4] S. Sanayei and A. Nosratinia, "Opportunistic downlink transmission with limited feedback," *IEEE Trans. Inf. Theory*, vol. 53, pp. 4363-4372, Nov. 2007.
- [5] J. Chen, R. A. Berry, and M. L. Honig, "Limited feedback schemes for downlink OFDMA based on sub-channel groups," *IEEE J. Sel. Areas Commun.*, vol. 26, pp. 1451-1461, Oct. 2008.

- [6] P. Svedman, S. K. Wilson, L. J. Cimimi, and B. Ottersten, "Opportunistic beamforming and scheduling for OFDMA systems," *IEEE Trans. Commun.*, vol. 55, pp. 941–952, May 2007.
- [7] Y. J. Choi and S. Bahk, "Selective channel feedback mechanisms for wireless multichannel scheduling," in *IEEE Intl. Symp. World of Wireless Mobile and Multimedia Networks (WoWMoM)*, pp. 289–300, Jun. 2006.
- [8] D. Tse and P. Vishwanath, *Fundamentals of Wireless Communications*. Cambridge University Press, 2005.
- [9] K. I. Pedersen, G. Monghal, I. Z. Kovacs, T. E. Kolding, A. Pokharyal, F. Frederiksen, and P. Mogensen, "Frequency domain scheduling for OFDMA with limited and noisy channel feedback," in *Proc. VTC (Fall)*, pp. 1792–1796, Oct. 2007.
- [10] A. Pokharyal, T. E. Kolding, and P. E. Mogensen, "Performance of downlink frequency domain packet scheduling for the UTRAN Long Term Evolution," in *Proc. PIMRC*, Sep. 2006.
- [11] S. T. Chung and A. J. Goldsmith, "Degrees of freedom in adaptive modulation: A unified view," *IEEE Trans. Commun.*, vol. 49, pp. 1561–1571, Jan. 2001.
- [12] R. Kwan, C. Leung, and J. Zhang, "Multiuser scheduling on the downlink of an LTE cellular system," *Research Lett. Commun.*, Jan. 2008.
- [13] J. Leinonen, J. Hamalainen, and M. Juntti, "Performance analysis of downlink OFDMA resource allocation with limited feedback," *IEEE Trans. Veh. Technol.*, vol. 8, pp. 2927–2937, Jun. 2009.
- [14] S. Catreux, L. J. Greenstein, and V. Erceg, "Some results and insights on the performance gains of MIMO systems," *IEEE J. Sel. Areas Commun.*, vol. 21, pp. 839–847, Jun. 2003.
- [15] M. Torabi, D. Haccoun, and W. Ajib, "Performance analysis of scheduling schemes for rate-adaptive MIMO OSFBC-OFDM systems," *IEEE Trans. Veh. Technol.*, vol. 59, pp. 2363–2379, Jun. 2010.
- [16] "Evolved universal terrestrial radio access (E-UTRA); physical layer procedures (release 8)," Tech. Rep. 36.213 (v8.3.0), 3rd Generation Partnership Project (3GPP), 2008.
- [17] M. Assaad and A. Mourad, "New frequency-time scheduling algorithms for 3GPP/LTE-like OFDMA air interface in the downlink," in *Proc. VTC (Spring)*, pp. 1964–1969, May 2008.
- [18] Z. Lin, P. Xiao, and B. Vucetic, "SINR distribution for LTE downlink multiuser MIMO systems," in *Proc. ICASSP*, pp. 2833–2836, Apr. 2009.
- [19] S. Ko, S. Lee, H. Kwon, and B. G. Lee, "Mode selection-based channel feedback reduction schemes for opportunistic scheduling in OFDMA systems," *IEEE Trans. Wireless Commun.*, vol. 9, pp. 2842–2852, Sep. 2010.
- [20] J. Chen, R. A. Berry, and M. L. Honig, "Large system performance of downlink OFDMA with limited feedback," in *Proc. IEEE Int. Symp. Inf. Theory*, pp. 1399–1403, Jul. 2006.
- [21] J. G. Choi and S. Bahk, "Cell-throughput analysis of the proportional fair scheduler in the single-cell environment," *IEEE Trans. Veh. Technol.*, vol. 56, pp. 766–778, Mar. 2007.
- [22] S. Catreux, P. F. Driessen, and L. J. Greenstein, "Data throughputs using multiple-input multiple-output (MIMO) techniques in a noise-limited cellular environment," *IEEE Trans. Wireless Commun.*, vol. 1, pp. 226–235, Apr. 2002.
- [23] E. Dahlman, H. Ekstrom, A. Furuskar, Y. Jading, J. Karlsson, M. Lundvall, and S. Parkvall, "The 3G Long-Term-Evolution radio interface concepts and performance evaluation," in *Proc. VTC (Spring)*, pp. 137–141, May 2006.
- [24] U. Fernandez-Plazaola, E. Martos-Naya, J. F. Paris, and A. J. Goldsmith, "Adaptive modulation for MIMO systems with channel prediction errors," *IEEE Trans. Wireless Commun.*, vol. 9, pp. 2516–2527, Aug. 2010.
- [25] A. Nasri and R. Schober, "Performance of BICM-SC and BICM-OFDM systems with diversity reception in non-Gaussian noise and interference," *IEEE Trans. Wireless Commun.*, vol. 57, pp. 3316–3327, Nov. 2009.
- [26] NTT DoCoMo, "Investigations on codebook size for MIMO precoding in E-UTRA downlink," *RI-070093, 3GPP RAN1 #47*, Jan. 2007.
- [27] NTT DoCoMo, Fujitsu, Mitsubishi Electric Corporation, NEC, QUALCOMM Europe, Sharp, Toshiba Corporation, "Adaptive modulation and channel coding rate control for single-antenna transmission in frequency domain scheduling," *RI-060039, 3GPP TSG-RAN WG1 LTE Ad Hoc Meeting*, Jan. 2006.
- [28] S. Lu, Y. Cai, L. Zhang, J. Li, P. Skov, C. Wang, and Z. He, "Channel-aware frequency domain packet scheduling for MBMS in LTE," in *Proc. VTC (Spring)*, Apr. 2009.
- [29] H. Song, R. Kwan, and J. Zhang, "General results on SNR statistics involving EESM-based frequency selective feedbacks," *IEEE Trans. Wireless Commun.*, vol. 9, pp. 1790–1798, May 2010.
- [30] A. Jalali, R. Padovani, and R. Pankaj, "Data throughput of CDMA-HDR a high efficiency-high data rate personal communication wireless system," in *Proc. VTC (Spring)*, pp. 1854–1858, May 2000.
- [31] A. M. Tulino and S. Verdú, *Random Matrix Theory and Wireless Communications*. Now Publishers Inc., 2004.
- [32] M. Abramowitz and I. Stegun, *Handbook of mathematical functions with formulas, graphs, and mathematical tables*. Dover, 9 ed., 1972.
- [33] K. L. Baum, T. A. Kostas, P. J. Sartori, and B. K. Classon, "Performance characteristics of cellular systems with different link adaptation strategies," *IEEE Trans. Veh. Technol.*, vol. 52, pp. 1497–1507, Nov. 2003.
- [34] T. Starr, J. M. Cioffi, and P. J. Silverman, *Understanding Digital Subscriber Line Technology*. Prentice Hall PTR, 1 ed., 1999.
- [35] R. Love, R. Kuchibhotla, A. Ghosh, R. Ratasuk, B. Classon, and Y. Blankenship, "Downlink control channel design for 3GPP LTE," in *Proc. WCNC*, pp. 813–818, Apr. 2008.
- [36] J. P. Kermaol, L. Schumacher, K. I. Pedersen, P. E. Mogensen, and F. Frederiksen, "A stochastic MIMO radio channel model with experimental validation," *IEEE J. Sel. Areas Commun.*, vol. 20, pp. 1211–1226, Aug. 2002.
- [37] ITU-R, "Guidelines for evaluation of radio interface technologies for IMT-advanced," *M.2135-1*, 2009.
- [38] S. N. Donthi and N. B. Mehta, "Performance analysis of subband-level channel quality indicator feedback scheme of LTE," in *Proc. Nat. Conf. Commun.*, Jan. 2010.
- [39] A. F. Molisch, M. Z. Win, and J. H. Winters, "Reduced-complexity transmit/receive-diversity systems," *IEEE Trans. Signal Process.*, vol. 51, pp. 2729–2738, Nov. 2003.

PLACE  
PHOTO  
HERE

development for 3G handsets. His research interests include the design and analysis of algorithms for wireless cellular systems, communication networks and MIMO systems.

PLACE  
PHOTO  
HERE

**Sushruth N. Donthi** received his Bachelor of Engineering degree in Telecommunications Engineering from Vemana Institute of Technology, Bangalore in 2006. He received his Master of Science degree from the Dept. of Electrical Communication Engineering, Indian Institute of Science, Bangalore, India in 2011. Since then, he has been with Broadcom Communications Technologies Pvt. Ltd., Bangalore, India working on design and implementation of parts of the LTE protocol stack. From 2006–2008, he was at LG Soft India Pvt. Ltd., working on software development for 3G handsets. His research interests include the design and analysis of algorithms for wireless cellular systems, communication networks and MIMO systems.

**Neelesh B. Mehta** (S'98-M'01-SM'06) received his Bachelor of Technology degree in Electronics and Communications Engineering from the Indian Institute of Technology (IIT), Madras in 1996, and his M.S. and Ph.D. degrees in Electrical Engineering from the California Institute of Technology, Pasadena, CA in 1997 and 2001, respectively. He is now an Assistant Professor at the Dept. of Electrical Communication Engineering, Indian Institute of Science (IISc), Bangalore, India. Prior to joining IISc, he held research scientist positions in the Wireless Systems Research group in AT&T Laboratories (NJ, USA), Broadcom Corp. (NJ, USA), and Mitsubishi Electric Research Laboratories (MA, USA). His research includes work on link adaptation, multiple access protocols, system-level performance analysis of cellular systems, MIMO and antenna selection, and cooperative communications. He was also actively involved in radio access network physical layer (RAN1) standardization activities in 3GPP. He has served on several TPCs. He was a TPC co-chair for WISARD 2010 and 2011 workshops, National Conference on Communications (NCC) 2011, Transmission technologies track of VTC 2009 (Fall), Frontiers of Networking and Communications symposium of Chinacom 2008, and the tutorials co-chair for SPCOM 2010. He is an Editor of the IEEE Transactions on Wireless Communications and an executive committee member of the IEEE Bangalore Section and the Bangalore chapter of the IEEE Signal Processing Society.